Estuarine, Coastal and Shelf Science 204 (2018) 164–176

Contents lists available at ScienceDirect

Estuarine, Coastal and Shelf Science

journal homepage: www.elsevier.com/locate/ecss

Terrestrial laser scanning to quantify above-ground biomass of structurally complex coastal wetland vegetation

Christopher J. Owers*, Kerrylee Rogers, Colin D. Woodroffe

GeoQuEST Research Centre, School of Earth and Environmental Sciences, University of Wollongong, Wollongong, Australia

ARTICLE INFO

Article history:
Received 12 December 2017
Received in revised form
15 February 2018
Accepted 24 February 2018
Available online 2 March 2018

Keywords:
Vegetation structure
Mangrove
Saltmarsh
Biomass
Carbon storage
Allometric equations

ABSTRACT

Above-ground biomass represents a small yet significant contributor to carbon storage in coastal wetlands. Despite this, above-ground biomass is often poorly quantified, particularly in areas where vegetation structure is complex. Traditional methods for providing accurate estimates involve harvesting vegetation to develop mangrove allometric equations and quantify saltmarsh biomass in quadrats. However broad scale application of these methods may not capture structural variability in vegetation resulting in a loss of detail and estimates with considerable uncertainty. Terrestrial laser scanning (TLS) collects high resolution three-dimensional point clouds capable of providing detailed structural morphology of vegetation. This study demonstrates that TLS is a suitable non-destructive method for estimating biomass of structurally complex coastal wetland vegetation. We compare volumetric models, 3-D surface reconstruction and rasterised volume, and point cloud elevation histogram modelling techniques to estimate biomass. Our results show that current volumetric modelling approaches for estimating TLS-derived biomass are comparable to traditional mangrove allometrics and saltmarsh harvesting. However, volumetric modelling approaches oversimplify vegetation structure by underutilising the large amount of structural information provided by the point cloud. The point cloud elevation histogram model presented in this study, as an alternative to volumetric modelling, utilises all of the information within the point cloud, as opposed to sub-sampling based on specific criteria. This method is simple but highly effective for both mangrove ($r^2 = 0.95$) and saltmarsh ($r^2 > 0.92$) vegetation. Our results provide evidence that application of TLS in coastal wetlands is an effective non-destructive method to accurately quantify biomass for structurally complex vegetation.

1. Introduction

Coastal ecosystems, particularly mangrove and saltmarsh, provide essential ecosystem services that have widespread benefits at local and global scales (Ewel et al., 1998; Barbier et al., 2011; Zelder and Kercher, 2005; Lee et al., 2014). In particular, these 'blue carbon' ecosystems reportedly sequester more atmospheric carbon per unit area than any other natural ecosystem in the world (Duarte et al., 2005; McLeod et al., 2011; Alongi, 2014). Increasing awareness of the need to attempt to mitigate the effects of climate change has led to the inclusion of coastal ecosystems in national carbon accounts and offset initiatives such as Reducing Emissions from Deforestation and Forest Degradation (REDD+) (Alongi et al., 2015; Sutton-Grier and Moore, 2016; Kelleway et al., 2017). However, carbon storage services provided by blue carbon ecosystems are not spatially homogeneous, varying in response to factors operating at a range of scales (Twilley et al., 1992; Kelleway et al., 2016; Owers et al., 2016a; Yando et al., 2016; Macreadie et al., 2017). Inclusion of coastal ecosystems in national carbon accounts and offset initiatives requires accurate assessment of carbon storage. This is particularly important to facilitate and validate broad-scale mapping relevant for national and regional assessments of biomass and above-ground carbon storage (Gibbs et al., 2007; Chave et al., 2014).

Providing accurate estimates of above-ground biomass in coastal wetlands has traditionally involved destructive harvesting of vegetation (Kauffman and Donato, 2012; Howard et al., 2014). For mangrove, allometric equations are commonly developed by harvesting a subset of mangroves of a particular species with a specific geographical area, and correlating measured parameters from harvested trees, such as height, diameter at breast height (DBH) and crown area, to above-ground biomass (Komiyama et al., 2008). For saltmarsh vegetation, above-ground biomass is determined by

* Corresponding author.
E-mail address: cjo766@uowmail.edu.au (C.J. Owers).

https://doi.org/10.1016/j.ecss.2018.02.027
0272-7714/

harvesting a small area of particular species, typically on the basis of replicate quadrats (Howard et al., 2014). Allometric equations have been developed for saltmarsh using stem height (Thursby et al., 2002; Craft, 2013); however, this approach is impractical for many saltmarsh species that do not show strong relationships between height and growth.

In addition to clear detrimental consequences of destructive harvesting, particularly given the conservation status of mangrove and saltmarsh, developing allometric equations for mangrove and averaging biomass of harvested saltmarsh replicates may not provide a reasonable level of accuracy, as previously suggested (Soares and Schaeffer-Novelli, 2005; Estrada et al., 2014). Allometric equations developed for mangrove often do not capture the full range of morphological growth required for a particular species and geographic area, resulting in limited application or extrapolation resulting in substantial uncertainty (Kauffman and Donato, 2012; Bonham, 2013; Olagoke et al., 2015). Saltmarsh biomass can vary markedly in areas with high species diversity, where mosaicked distribution in the landscape results in variable densities associated with salinity and inundation gradients (Clarke, 1993; Clarke and Jacoby, 1994; Saintilan, 2009). Variability in biomass may be more pronounced in regions where mangrove and saltmarsh vegetation are structurally complex, particularly in temperate regions where they coexist (Owers et al., in review; Morrisey et al., 2010; Owers et al., 2016b).

Terrestrial laser scanning (TLS) is a technique that uses a ground-based active remote sensor that collects high resolution three-dimensional point clouds capable of providing detailed structural morphology of vegetation (Newnham et al., 2015). TLS has been demonstrated to effectively measure biomass in forested and pasture environments, providing clear benefits over traditional biomass measures as it is non-destructive and captures a level of detail that cannot be achieved using traditional methods (Olsoy et al., 2014; Calders et al., 2015; Greaves et al., 2015; Paynter et al., 2016; Cooper et al., 2017; Wallace et al., 2017). However, current modelling approaches to measure biomass using TLS have been criticised for oversimplifying vegetation structure and underutilising the point cloud (Newnham et al., 2015).

For large trees, biomass has been estimated using TLS by deriving trunk and branch volume, modelled using cylindrical shapes, and multiplying by wood specific gravity (Hackenberg et al., 2015a; Stovall et al., 2017). This rudimentary shape fitting may oversimplify tree architecture, particularly where structure is complex. Furthermore, non-woody biomass has rarely been considered in TLS estimates (i.e. Belton et al., 2013; Calders et al., 2013, 2015; Raumonen et al., 2013; Kaasalainen et al., 2014; Olagoke et al., 2015). For shrub vegetation, modelling the general shape of the whole plant using 3-D surface reconstructions is common, whereby scanned samples are destructively harvested to establish relationships between volume and biomass (Olsoy et al., 2014, Osloy et al., 2016; Greaves et al., 2015). This method, though relatively simple to execute, under-utilises the point cloud and results in over-simplifying vegetation structure. Similarly, current modelling approaches for grass and pasture species limits capacity to detect variation in density. A rasterised volumetric approach, whereby grass volume is calculated using two modelled layers from the point cloud, assumes full density of biomass relative to vegetation height. Linear models relating volume to harvested biomass have produced varying results and are likely limited by assumptions of vegetation density associated with the modelling approach (see Loudermilk et al., 2009; Eitel et al., 2014; Greaves et al., 2015; Cooper et al., 2017).

The application of TLS for estimating biomass should exploit the large amount of structural information obtained (Newnham et al., 2015). Current volumetric modelling approaches sub-sample the point cloud, resulting in considerable loss of detail. An alternative approach to volumetric modelling is statistical analysis of the point cloud elevation histogram to establish relationships with above-ground biomass. This approach maximises utilisation of the information provided by the point cloud, avoiding over-simplification, reducing computational time, and does not require extensive modelling to extract volume. Statistical analysis of the point cloud elevation histogram has been explored, demonstrating promising preliminary results (i.e. Hauglin et al., 2013; Kankare et al., 2013; Srinivasan et al., 2014; Edwards, 2016; Rahman et al., 2017).

There have been few TLS applications in coastal wetlands in comparison to terrestrial ecosystems. Modelling saltmarsh biomass has been attempted however with limited success (Edwards, 2016). For mangrove, previous research has established TLS as a viable alternative to harvesting for developing allometric equations to estimate biomass (Feliciano et al., 2014; Olagoke et al., 2015). These studies use volumetric modelling to determine mangrove woody biomass and present results showing high agreement between TLS-derived biomass and allometric estimates. However, both studies are limited to tall and relatively straight tropical mangrove stands, whereby tree morphology is somewhat simpler than can be observed for mangrove at latitudinal extremes where trees can be multi-stemmed, shrub-like and dwarfed (Morrisey et al., 2010; Owers et al., 2016b). Accordingly, the structure of mangrove in these studies is relatively well described, despite under-utilising the point cloud. Furthermore, no attempt to model non-woody biomass is given, limiting the adoption of TLS for mangrove biomass.

The aim of this study was to apply different methods using TLS to estimate biomass of structurally complex coastal wetland vegetation. The specific methods tested include 3D surface reconstruction of mangrove and the saltmarsh shrub *Tecticornia arbuscula*, rasterised volume modelling of grass, rush, and herbs and forbs saltmarsh, and statistical analysis of point cloud elevation histograms, hereafter known as the point cloud elevation histogram model, to establish relationships with biomass of mangrove and saltmarsh. Our hypothesis was that methods using TLS data will give comparable above-ground biomass estimates as traditional mangrove allometric and saltmarsh vegetation harvesting techniques. Using TLS-derived point clouds of mangrove and saltmarsh vegetation the specific objectives of this study are to:

1. Determine vegetation volume and biomass for mangrove and *Tecticornia arbuscula* by applying 3-D surface reconstruction models to the point cloud that are validated against biomass estimates derived using traditional allometric equations and harvesting techniques.
2. Determine vegetation volume for grasses (*Sporobolus virginicus*), rushes (*Juncus kraussii*), and herbs and forbs (*Samolus repens*, *Sarcocornia quinqueflora*) saltmarsh using a rasterised volumetric approach, and correlate biomass estimates derived using traditional harvesting techniques.
3. Establish relationships between point cloud elevation histograms and biomass derived from traditional techniques to develop an alternative TLS-derived biomass model.
4. Compare volumetric models, 3-D surface reconstruction and rasterised volume, and point cloud elevation histogram modelling techniques with biomass estimates derived using traditional techniques.

As an outcome of this study we develop a modelling technique that provides accurate non-destructive estimates of biomass in coastal wetlands. This is particularly important given the conservation status of coastal ecosystems within many jurisdictions globally; to avoid traditional techniques that require harvesting of

vegetation, and to establish biomass inventories with the required confidence necessary for trading in carbon markets.

2. Methods

2.1. Study area

Southeast Australia has a wave-dominated coastline. Extensive saline coastal wetlands are restricted to estuaries and coastal embayments where low energy hydrodynamic conditions are suitable for establishment and growth (Roy et al., 2001). The temperate climate of southeast Australia supports mangrove and saltmarsh communities, these co-occur along intertidal shorelines (Adam, 1990). These vegetation communities exhibit strong zonation associated with tidal range, commonly occurring above mean sea level. Mangroves typically occur lower within the tidal frame, while saltmarsh occupy higher intertidal areas. The latitudinal range of this study is 32° S to 39° S. Data were collected from several sites in this region; Hexham swamp (32°51′ S, 151°41′ E), Minnamurra River (34°38′ S, 150°51′ E), Currambene Creek (35°1′ S, 150°40′ E), Kooweerup (38° 13′ S 145° 24′ E), and Rhyll (38° 27′ S 145° 17' E). *Avicennia marina* is the dominant mangrove species in the region. *Aegiceras corniculatum* is also present in small patches of specific inundation and salinity. These species of mangrove exhibit three dominant structural forms within the region (Fig. 1 a–c). Tall mangrove were typically 3 m–8 m in height with a diameter at breast height (DBH) greater than 15 cm. Shrub mangrove were typically 1.3 m–3 m in height with a DBH less than 15 cm. Dwarf mangrove were typically less than 1.3 m in height (Owers et al., 2016b). *Avicennia marina* is present in all three dominant structural forms; however *Aegiceras corniculatum* is only present in dwarf mangrove. Commonly present saltmarsh species are *Sporobolus virginicus*, *Samolus repens*, *Juncus kraussii*, *Tecticornia arbuscula*, and *Sarcocornia quinqueflora* (Fig. 1 d–h) (Clarke, 1993; Sainty et al., 2012).

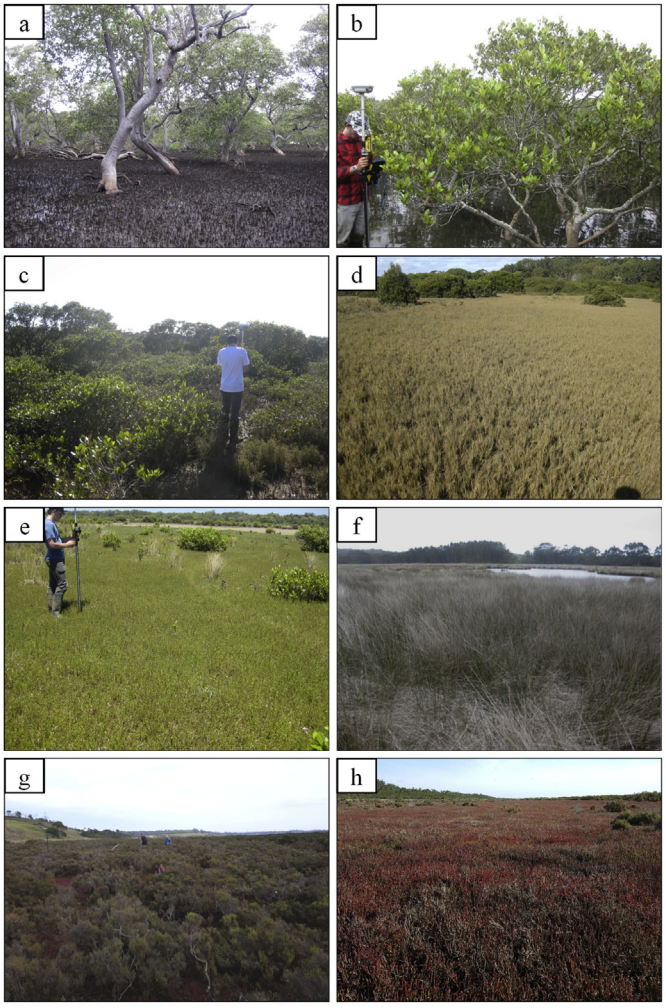

Fig. 1. Field photo examples of mangrove structural form and saltmarsh species present in the region; (*a*) tall mangrove, *b*) shrub mangrove, *c*) dwarf mangrove, *d*) *Sporobolus virginicus*, *e*) *Samolus repens*, *f*) *Juncus kraussii*, *g*) *Tecticornia arbuscula*, *h*) *Sarcocornia quinqueflora*.

2.2. Terrestrial laser scanning of mangrove and saltmarsh

TLS data capture was completed using a Leica ScanStation C10 (Table S1). Locations of scans and positions of reflective targets were strategically placed to avoid obstructions to scanning selected mangroves or saltmarsh quadrats, as well as ensuring sufficient survey redundancy for satisfactory registration of point clouds (Fig. S1). All scans were completed at low tide to ensure comprehensive data capture of vegetation. Due to uneven and unstable wetland surfaces the tripod stand and reflective targets were mounted on steel posts with a custom designed faceplate to ensure a stable level before scanning (Fig. S1). Hemispherical photos were automatically acquired after the scan was complete.

Once acquired, each scan was registered using the reflective targets to create a single point cloud in the Leica software package Cyclone 9.1. Root mean square error (RMSE) was below 0.03 m for all registered point clouds and all points were colourised based on the hemispherical photos. A total of 53 mangroves were scanned from various sites including 17 tall mangrove, 30 shrub mangrove and 6 dwarf mangrove. All scanned mangroves were *Avicennia marina*. A range of saltmarsh species in varying stand densities were scanned. These were *Sporobolus virginicus*, *Samolus repens*, *Juncus kraussii*, *Tecticornia arbuscula*, and *Sarcocornia quinqueflora*. Selected mangrove and *Tecticornia arbuscula* individual plants were extracted manually from the point cloud as well as selected saltmarsh quadrats (25 × 25 cm) for *Sporobolus virginicus*, *Samolus repens*, *Juncus kraussii* and *Sarcocornia quinqueflora*.

2.3. Above-ground biomass derived from traditional techniques

Each scanned mangrove was measured for height (cm), crown area (m^2), and diameter of the stem(s) (cm). Structure-specific allometric equations were used to calculate above-ground biomass (AGB) of each mangrove (Owers et al., in review). Woody AGB, leaf plus inflorescence AGB and total AGB were calculated for each mangrove. Equations are given in Table S2.

Saltmarsh vegetation was harvested to determine above-ground biomass. Five individual *Tecticornia arbuscula* plants were harvested, differing in height and crown area to capture a range of growth morphologies. Scanned saltmarsh quadrats (25 × 25 cm) of *Sporobolus virginicus*, *Samolus repens*, *Juncus kraussii* and *Sarcocornia quinqueflora* were harvested in high, medium and low density stands. Four replicates were harvested in each stand density. All harvested material was transferred to the laboratory. Vegetation was rinsed to remove excess sediment, weighed, then oven dried at 60 °C to a constant mass and reweighed.

2.4. Mangrove 3-D modelling

TLS-derived volume for mangrove vegetation was determined by applying 3-D surface reconstruction models to the point cloud.

Several 3-D surface reconstruction models were applied to compare volume estimates between mangrove individuals (Fig. 2).

Due to structurally complex mangrove, two methods were employed for TLS-derived mangrove volume. Where woody compartments could be automatically extracted, woody and non-woody compartments were modelled separately (Fig. 2 b, c). This included all tall mangrove and several larger shrub mangrove. Automatic extraction of woody and non-woody compartments was completed using the toolset *Extract Major Branches* in the open source software package Computree using the Simpletree plugin (Hackenberg et al., 2015b). This toolset uses principal components analysis with user set eigenvalue thresholds to define a point as stem or twig by analysing the neighbourhood of each point in the point cloud (Raumonen et al., 2013; Hackenberg et al., 2015b). However, where woody compartments could not be automatically extracted, due to occlusion by non-woody compartments, mangrove compartments were not modelled separately. This included shrub mangrove and all dwarf mangrove.

Volumes of woody compartments were calculated using two 3-D surface reconstruction models; quantitative structure models (QSM) and Poisson surface reconstruction (Fig. 2 d, e). QSMs are based on cylinders that define the trunk and branches through a regression algorithm (Raumonen et al., 2013). Poisson surface reconstruction is a triangular mesh generation algorithm that is particularly useful with highly noisy data (Kazhdan and Hoppe, 2013). Volume of non-woody compartments were calculated using two 3-D surface reconstruction models; Poisson surface reconstruction and convex hull (Fig. 2 f, g). The convex hull model is a triangular mesh generation algorithm that represents the smallest surface area that contains all points in the point cloud (Barber et al., 1996; Olsoy et al., 2014; Stovall et al., 2017). The same approach for calculating volume using Poisson and convex hull 3-D surface reconstruction models was used for small stature mangrove where woody compartments were occluded by non-woody compartments and could not be modelled separately (Fig. 2 i, j). Analysis of variance (ANOVA) was used to establish relationships between TLS-derived volume estimates for woody and non-woody compartments, as well as small stature mangroves, using different 3-D surface reconstruction models. All statistical tests completed in this study were carried out using a 0.05 level of significance.

Above-ground biomass of mangrove for woody compartments was calculated by multiplying the volume, determined by 3-D surface reconstruction models, by wood specific gravity of each mangrove structure typical of southeast Australia (Tall mangrove = 0.774 g/cm^3, Shrub mangrove = 0.734 g/cm^3) (Owers et al., in review). For non-woody compartments and small stature mangroves above-ground biomass could not simply be calculated by applying a density factor. Rather, 3-D surface reconstruction volumes were converted to 'crown volume' (height x crown area). An average ratio was determined for this conversion for both Poisson-derived volumes and convex hull-derived volumes for non-woody compartments and small stature mangroves. These ratios were then used to estimate Poisson and convex hull volumes for harvested mangroves from Owers et al. (in review). A total of 43 mangroves were harvested.

Above-ground biomass of woody and non-woody compartments was determined for each harvested mangrove. Allometric equations were developed to estimate above-ground biomass of scanned mangroves using 3-D surface reconstruction volumes of Poisson and convex hull. Dependent variables were leaves plus inflorescence biomass and total biomass. Independent variables were Poisson-derived and convex hull-derived volumes. Response and independent variables were natural log (ln) transformed prior to analysis to achieve assumptions of normality. Developed equations were back transformed from log transformation to facilitate calculating dependent variables. A correction factor (CF) was calculated for all equations as back transformations from log transformations are associated with underestimation of response variables (Sprugel, 1983). CF is calculated as exp(RMSE/2). Allometric equations are in the form:

$$\ln(y) = a + b \times \ln(x) \quad (1)$$

where y is the biomass, and a and b are constants. To establish the

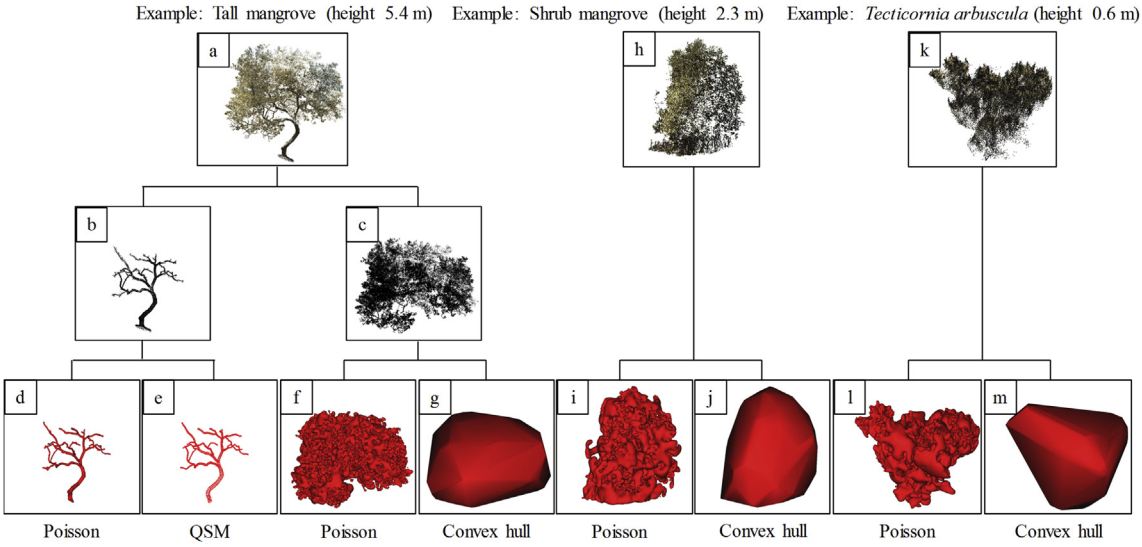

Fig. 2. Workflow for TLS-derived volume for mangrove and *Tecticornia arbuscula* saltmarsh. For a) mangrove where b) woody and c) non-woody compartments could be automatically delineated, the woody compartment was modelled by comparing 3-D surface reconstruction methods d) Poisson reconstruction and e) quantitative structure models. The non-woody compartment was modelled by comparing 3-D surface reconstruction methods f) Poisson reconstruction and g) convex hull reconstruction. Where mangrove woody compartments were h) occluded by non-woody compartments and could not be automatically extracted, the point cloud was modelled similar to non-woody compartments; 3-D surface reconstruction techniques were compared for i) Poisson reconstruction and j) convex hull reconstruction. For k) *Tecticornia arbuscula*, the same workflow was undertaken as for non-woody compartments, l) Poisson reconstruction and m) convex hull reconstruction.

biomass and incorporate the correction factor, equation (1) is written as:

$$y = (\exp(a + b \times \ln(x))) \times CF \quad (2)$$

Statistical analysis for linear regression models, including coefficient of determination (r^2), root mean square error (RMSE) and statistical significance, was undertaken in JMP Version 11 (SAS Institute Inc., Cary, NC, USA).

TLS-derived above-ground biomass estimates of mangrove were compared with above-ground biomass estimates from allometric equations developed in Owers et al., (in review). ANOVA was used to identify significant differences between estimates for woody and non-woody compartments as well as total above-ground biomass. Mean confidence intervals (95%) were calculated for biomass derived from allometric equations for each scanned mangrove.

2.5. Tecticornia arbuscula 3-D modelling

Saltmarsh volumetric calculations for *Tecticornia arbuscula* were similar to the approach for mangrove non-woody compartments. *Tecticornia arbuscula* were structurally similar to dwarf mangrove and often the woody compartment was occluded by the non-woody components. Volume was calculated with Poisson and convex hull reconstruction models (Fig. 2 l, m). Analysis of variance (ANOVA) was used to compare TLS-derived volumes from different 3-D surface reconstructions.

Above-ground biomass, estimated using traditional harvesting techniques, was correlated with TLS-derived volume estimates of Poisson and convex hull 3-D surface reconstructions. The relationship between above-ground biomass and TLS-derived volume was tested using a range of models. The selected model was chosen where the relationship was significant ($p < 0.05$) and r^2 was optimised.

2.6. Saltmarsh rasterised volume modelling

TLS-derived volume for grasses (*Sporobolus virginicus*), rushes (*Juncus kraussii*), and herbs and forbs (*Samolus repens*, *Sarcocornia quinqueflora*) saltmarsh was determined using the rasterised volumetric approach developed by Loudermilk et al. (2009). This methodology involves a volumetric surface differencing approach whereby a raster grid is generated at a specified cell size and volume is calculated by summing the volumes of all cells within the quadrat. Two layers are required to be defined before calculating; the ground surface, or digital elevation model (DEM) and the canopy surface, or digital surface model (DSM). The ground surface was calculated as a planar model of the minimum points of the point cloud, as change in topography for small plots is suggested to be minimal (Cooper et al., 2017; Wallace et al., 2017). Two canopy surface models were calculated for analysis in this study, first using the maximum height of each cell and second using the average height of each cell. We tested this methodology for each species with differing cell sizes (1 cm, 2 cm, 5 cm) for both maximum height and average height, with interpolation between empty cells (if any) and no interpolation between empty cells, as has been tested in previous studies in different environments (Eitel et al., 2014; Cooper et al., 2017; Wallace et al., 2017). ANOVA was used to determine if cell size and interpolation of raster DSM had a significant effect on volume.

Volume estimates were correlated with biomass estimates derived from traditional harvesting techniques. Linear regressions were compared for above-ground biomass and TLS-derived volumes. Models were selected for each species where the relationship was significant ($p < 0.05$) and r^2 was optimised.

2.7. Point cloud elevation histogram to biomass model

An alternate model was developed that did not require modelling volume of the point cloud. Rather, all points in the point cloud for each mangrove/*Tecticornia arbuscula* individual and saltmarsh quadrat were used to develop point cloud elevation histograms (Fig. 3). Descriptive parameters were calculated for each point cloud. These were mean, standard deviation, range, median, median absolute deviation, number of points in point cloud, summation of points in point cloud (point elevation x n), variance, skewness and kurtosis. These parameters were selected as they represent the distribution of the point cloud histogram.

Linear models were developed using the histogram descriptive parameters (independent variables) and above-ground biomass (dependent variable) derived from traditional allometric and harvest techniques. A stepwise linear regression model was used to explore all models and combinations of independent variables. Separate linear models were developed for each mangrove and saltmarsh species. All samples were used in model development due to limited sample size. A model was selected for each species where the Bayesian information criterion (BIC) was optimised and the equation was significant ($p < 0.1$). Although other parameters have been used for model selection (i.e. r^2, AIC, RMSE), BIC was used in this study as it performs well with small data sets and penalises the addition of dependent variables (Pitt and Myung, 2002; Aertsen et al., 2010; Fabozzi et al., 2014). Where BIC was similar between optimised models (i.e. ± 1), the equation where RMSE was optimised was selected.

2.8. Model comparison

The point cloud elevation histogram method was compared to the 3-D surface reconstruction model for mangrove and *Tecticornia arbuscula*, as well as the rasterised volumetric method for *Sporobolus virginicus*, *Samolus repens*, *Juncus kraussii* and *Sarcocornia quinqueflora*. Each model was used to estimate above-ground biomass and this was compared to biomass estimates of mangrove and saltmarsh using traditional allometric methods and vegetation harvesting techniques. Models were evaluated using r^2 and analysis of covariance (ANCOVA). Each model was evaluated independently using ANCOVA by comparing the regression model to the 1:1 regression (i.e. where observed and estimated biomass were the same). Models were optimised where r^2 was higher and the model was not significantly different to the 1:1 regression ($p > 0.05$).

3. Results

3.1. Mangrove 3-D modelling

TLS-derived volume of woody and non-woody compartments varied with 3-D surface reconstruction method. For woody compartments, variation between Poisson and QSM derived volume estimates was insignificant ($p = 0.9213$). However Poisson and Convex hull volume estimates for non-woody compartments were significantly different ($p = 0.0042$). Convex hull volume estimates were substantially higher than Poisson derived volume estimates for non-woody compartments. Likewise, convex hull volume estimates for small stature mangroves were significantly higher than Poisson volume estimates ($p < 0.0001$).

Allometric equations were developed to calculate biomass from TLS-derived volume estimates of non-woody compartments and small stature mangroves. Average ratios were determined for conversion of Poisson-derived volumes and convex hull-derived volumes for non-woody compartments (Poisson = 0.12 ± 0.05 m^3,

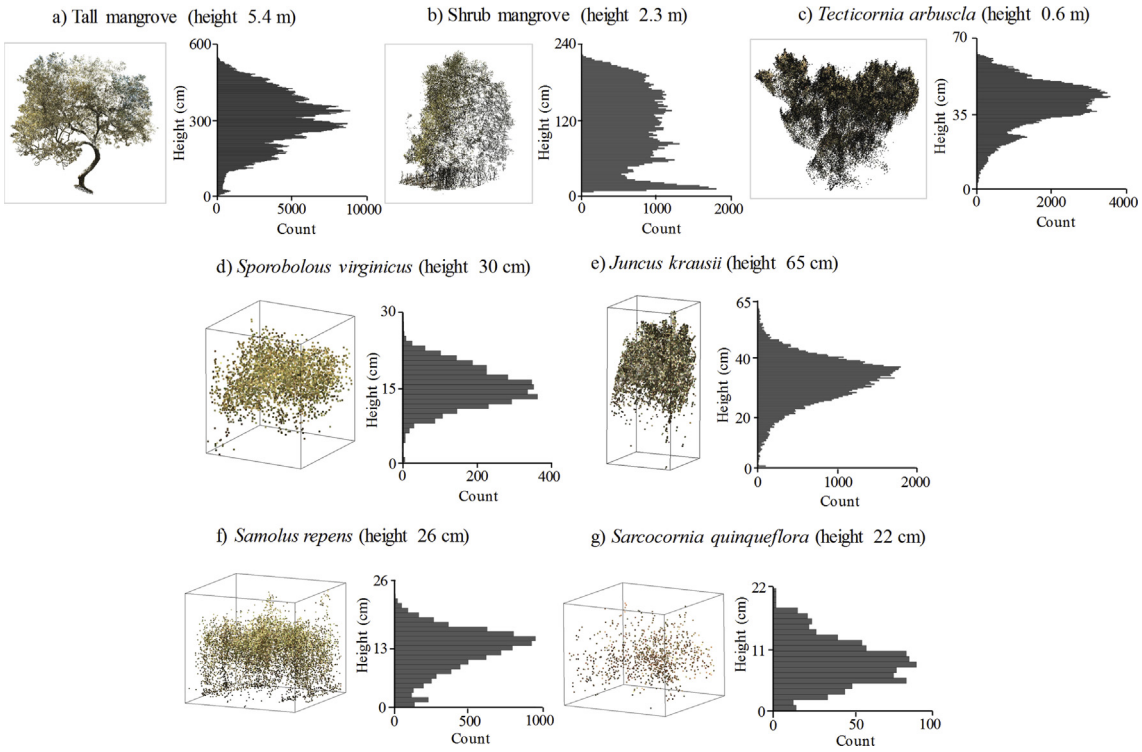

Fig. 3. Examples of TLS-derived point clouds of mangrove and saltmarsh vegetation and associated point cloud elevation histogram distributions. Elevation points are grouped into 5 cm bins for mangrove and 1 cm bins for saltmarsh.

Convex hull = 0.44 ± 0.16 m^3) and small stature mangroves (Poisson = 0.19 ± 0.07 m^3, Convex hull = 0.55 ± 0.16 m^3). Volume estimates from Poisson and convex hull surface reconstruction models were used as independent variables (Table 1). Robust equations were developed, however those developed for total above-ground biomass of small stature mangroves had greater r^2 and lower RMSE than leaf plus inflorescence developed for non-woody compartments.

TLS-derived above-ground biomass estimates were comparable with estimates from traditional allometric equations from Owers et al. (in review). Above-ground biomass estimated using allometric equations was not significantly different to TLS-derived biomass estimates for woody components (QSM p = 0.7235, Poisson p = 0.6511), non-woody components (Poisson p = 0.7758, convex hull p = 0.6931), or shorter stature mangroves (Poisson p = 0.9728, convex hull p = 0.9426). On average, TLS-derived woody compartment biomass estimates deviated from allometric estimates by 21% for QSM and 20% for Poisson. For non-woody compartments, average deviation from allometric estimates were greater in tall mangrove than shrub mangrove for both Poisson (tall mangrove 35%, shrub mangrove 25%) and convex hull (tall mangrove 30%, shrub mangrove 24%) derived estimates. Poisson and convex hull deviation from the allometric equation estimates was small for shorter stature mangroves; however shrub mangrove (Poisson 24%, convex hull 24%) had greater average deviation than dwarf mangrove (Poisson 17%, convex hull 13%).

A minority of TLS-derived biomass estimates were outside the 95% confidence interval of the allometric equation estimates (Fig. 4). For woody compartment estimates, one of 17 tall mangrove and one of 13 shrub mangrove measured was greater that then 95% confidence interval. This was similar for small stature mangrove where the majority of both shrub and dwarf mangrove TLS-derived estimates were within the 95% allometric confidence interval (shrub mangrove 16 of 17, dwarf mangrove 5 of 6). However, for non-woody compartments three of 17 tall mangrove were greater than the 95% confidence interval, as well as two of 13 shrub mangrove.

3.2. Tecticornia arbuscula 3-D modelling

The relationships between above-ground biomass of harvested *Tecticornia arbuscula* and TLS-derived volume estimates using 3-D

Table 1
Allometric equations for mangrove biomass from TLS-derived volumes. AGB (kg), Poisson volume (m^3), Convex hull volume (m^3). Equations should be calculated as y = (exp (a + b x ln(x_1))) x CF. *SE* Standard error of variable, *CF* correction factor, *n* sample size.

	AGB	Predictor (x_1)	a (SE)	b (SE)	Adj-r^2	RMSE	CF	n
Non-woody compartment	Leaves plus inflorescence	Poisson	0.4875 (0.0905)	0.9203 (0.0970)	0.79	0.47	1.1173	24
	Leaves plus inflorescence	Convex hull	−0.7143 (0.1511)	0.9203 (0.0970)	0.79	0.47	1.1173	24
Small stature mangrove	Total AGB	Poisson	2.0186 (0.1237)	1.1115 (0.0590)	0.92	0.43	1.0983	30
	Total AGB	Convex hull	0.8146 (0.0850)	1.1115 (0.0590)	0.92	0.43	1.0983	30

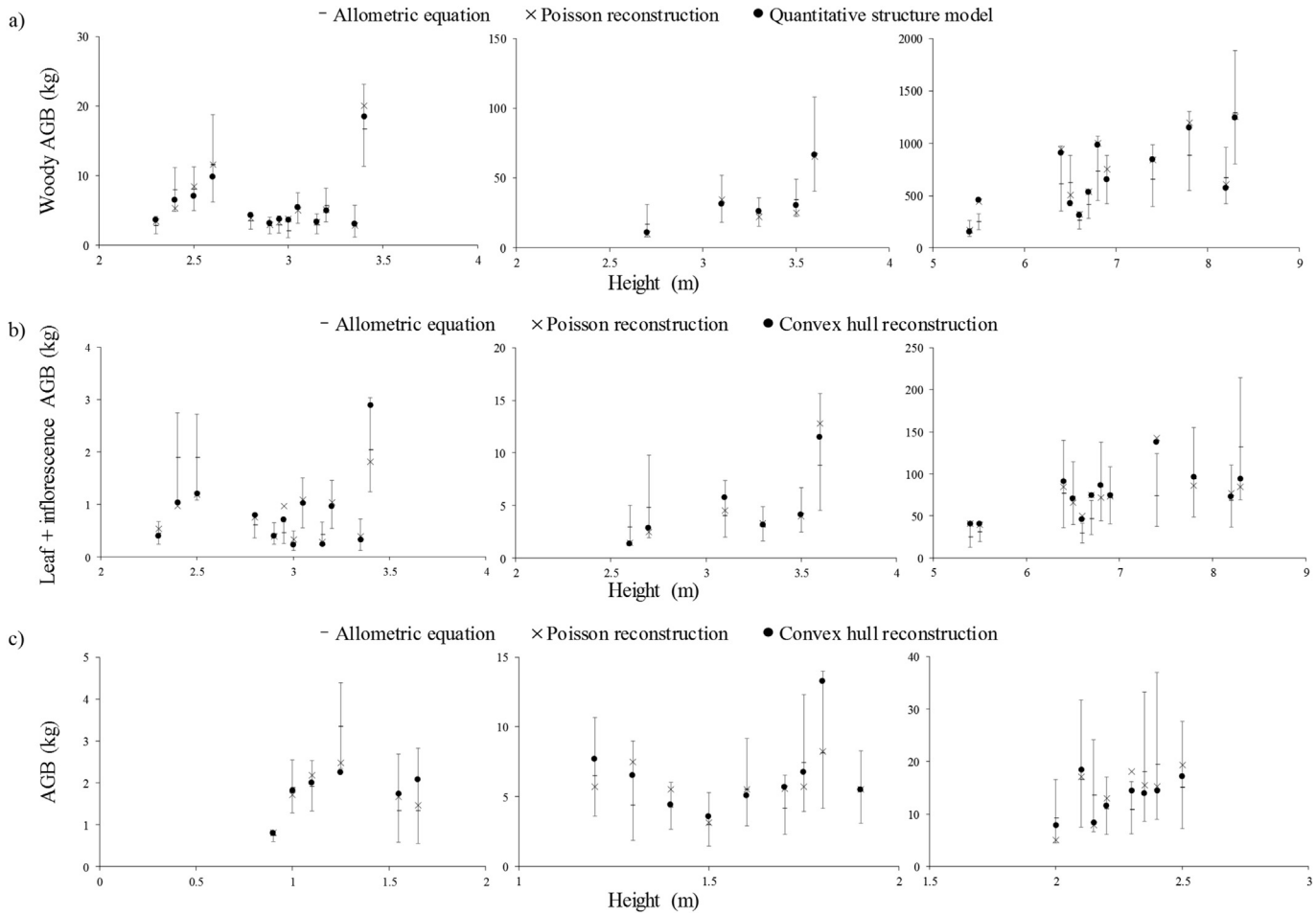

Fig. 4. Comparison of mangrove above-ground biomass estimates derived from allometry (error bars indicate 95% CI) and 3-D surface reconstruction models using TLS-derived point cloud. Where mangrove woody components could be delineated from the point cloud (i.e. tall and shrub mangrove) the a) woody and b) leaf plus inflorescence above-ground biomass were estimated separately. Where mangrove woody components could not be delineated from the point cloud (i.e. shrub and dwarf mangrove) due to occlusion, above-ground biomass was estimated for c) the entire plant. Note: graphs have overlapping axis due to sample heights that were similar with markedly different biomass. No sample has been repeated on overlapping graphs.

surface reconstruction were optimised using a logarithmic model (Fig. 5). Convex hull volume estimates were substantially higher than Poisson derived volume estimates, however this was insignificant ($p = 0.1284$). Both TLS-derived volume estimates had similar r^2 (Poisson $r^2 = 0.84$ $p = 0.0004$, Convex hull $r^2 = 0.84$ $p = 0.0005$).

3.3. Saltmarsh rasterised volume modelling

The optimal equation for three of the four saltmarsh species utilised the average height raster as the DSM for each saltmarsh quadrat. For *Sporobolus virginicus* and *Samolus repens* above-ground biomass was best described by 2 cm cell size, while for *Juncus kraussii* and *Sarcocornia quinqueflora* biomass was best described by 5 cm cell size (Table 2). *Samolus repens* had the highest r^2 and lowest RMSE of all species.

Interpolating empty cells of a raster did not significantly change the calculated volume for *Sporobolus virginicus*, *Samolus repens* or *Juncus kraussii*, irrespective of cell size or DSM used to calculate volume (p-value consistently > 0.05, Table S3). However, interpolating the DSM for *Sarcocornia quinqueflora* at a cell size of 1 cm did significantly modify volume calculations (maximum height $p = 0.0004$, average height $p = 0.0003$). Varying cell size for the rasterised volume method did significantly influence volume calculations for *Sporobolus virginicus*, *Samolus repens* and *Sarcocornia quinqueflora* (p-value consistently < 0.05, Table S4), whereby increasing the cell size increased calculated volume. However, this was not the case for *Juncus kraussii* (p-value consistently > 0.05, Table S4).

3.4. Point cloud elevation histogram to biomass model

Optimised point cloud elevation histogram models for mangrove and saltmarsh utilised greater than seven dependent variables to estimate AGB, with the exception of *Tecticornia arbuscula* (Table 3). Only *Juncus kraussii* utilised all descriptive parameters of the histogram as dependent variables. Common to all optimised models were the descriptive parameters of mean and range. All equations were significant ($p < 0.1$) with optimised BIC. The equation for *Samolus repens* had the lowest r^2, however r^2 for all species was greater than 0.9. For each addition of a dependent variable in stepwise linear regression modelling, the optimal equation was recorded (data in Table S9 – S14).

3.5. Model comparison

Above-ground biomass estimates using the point cloud elevation histogram method were compared with 3-D surface

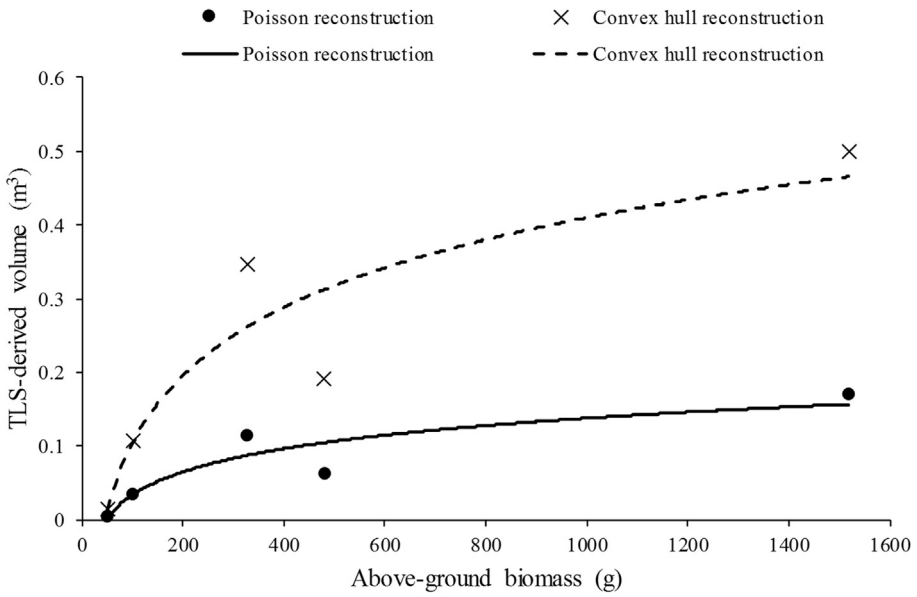

Fig. 5. Comparison of 3-D surface reconstruction models, Poisson and convex hull, and their relationships to above-ground biomass for harvested *Tecticornia arbuscula*.

Table 2
Optimised linear models for estimating above-ground biomass for each species of saltmarsh (*Sporobolus virginicus*, *Samolus repens*, *Juncus kraussii* and *Sarcocornia quinqueflora*) using the rasterised volume method. AGB (g). All linear models provided in Table S5 – S8.

Linear model for each species	Adj-r^2 (r^2)	RMSE	p
Sporobolus virginicus AGB = 332 + (75926 × 2 cm max height non interpolated)	0.46 (0.51)	384	0.0095
Juncus kraussii AGB = 685 + (17952 × 5 cm average height non interpolated)	0.42 (0.48)	494	0.0131
Samolus repens AGB = - 11 + (41267 × 5 cm average height non interpolated)	0.64 (0.67)	131	0.0012
Sarcocornia quinqueflora AGB = - 157 + (154384 × 2 cm average height interpolated)	0.56 (0.60)	254	0.0032

Table 3
Optimised point cloud elevation histogram linear models for mangrove AGB (kg) and saltmarsh AGB (g). Optimised linear models for each variable addition in stepwise model provided in Table S9 – S14.

Linear model for each species	BIC	Adj-r^2 (r^2)	RMSE	p
Mangrove (*A. marina*) AGB = −2.6 - (11 × mean) - (10 × standard deviation) - (0.0001 × number of points) + (0.0000004 × sum of points) + (0.02 × variance) + (8.9 × median) + (2.6 × range) + (3.8 × mean absolute deviation)	642	0.94 (0.95)	78	<0.0001
Tecticornia arbuscula AGB = 24 + (230 × mean) + (2376 × skewness) - (115 × range)	21	0.99 (0.99)	2.1	0.0022
Sporobolus virginicus AGB = −3184 + (1754 × mean) + (7846 × standard deviation) - (0.8 × number of points) - (335 × variance) - (4066 × skewness) - (4588 × kurtosis) - (2687 × median) + (791 × range) - (9906 × mean absolute deviation)	153	0.96 (0.99)	109	0.0356
Juncus kraussii AGB = −44254 + (1231 × mean) + (9852 × standard deviation) + (1.3 × number of points) - (0.01 × sum of points) - (290 × variance) + (17462 × skewness) + (2391 × kurtosis) + (945 × median) - (1931 × range) + (1902 × mean absolute deviation)	129	0.99 (0.99)	52	0.0589
Samolus repens AGB = 7191 - (370 × mean) - (3365 × standard deviation) + (0.03 × number of points) + (407 × variance) + (901 × skewness) + (510 × median) - (63 × range)	154	0.79 (0.92)	100	0.0412
Sarcocornia quinqueflora AGB = 3003 - (1726 × mean) - (2154 × standard deviation) - (2.7 × number of points) + (0.2 × sum of points) + (167 × variance) + (2113 × skewness) - (824 × kurtosis) + (1812 × median) + (122 × range)	155	0.90 (0.98)	120	0.0781

reconstruction estimates for mangrove and *Tecticornia arbuscula* and biomass estimates for *Sporobolus virginicus*, *Samolus repens*, *Juncus kraussii* and *Sarcocornia quinqueflora* using the rasterised volume method (Fig. 6). For mangrove, the AGB estimates of 3-D surface reconstructions were the average of the two 3-D surface reconstruction methods employed (QSM and Poisson for woody compartment; Poisson and convex hull for non-woody compartment). For mangrove where woody and non-woody compartments were delineated the average of the 3-D surface reconstruction methods was added together for total AGB. Similarly for *Tecticornia*

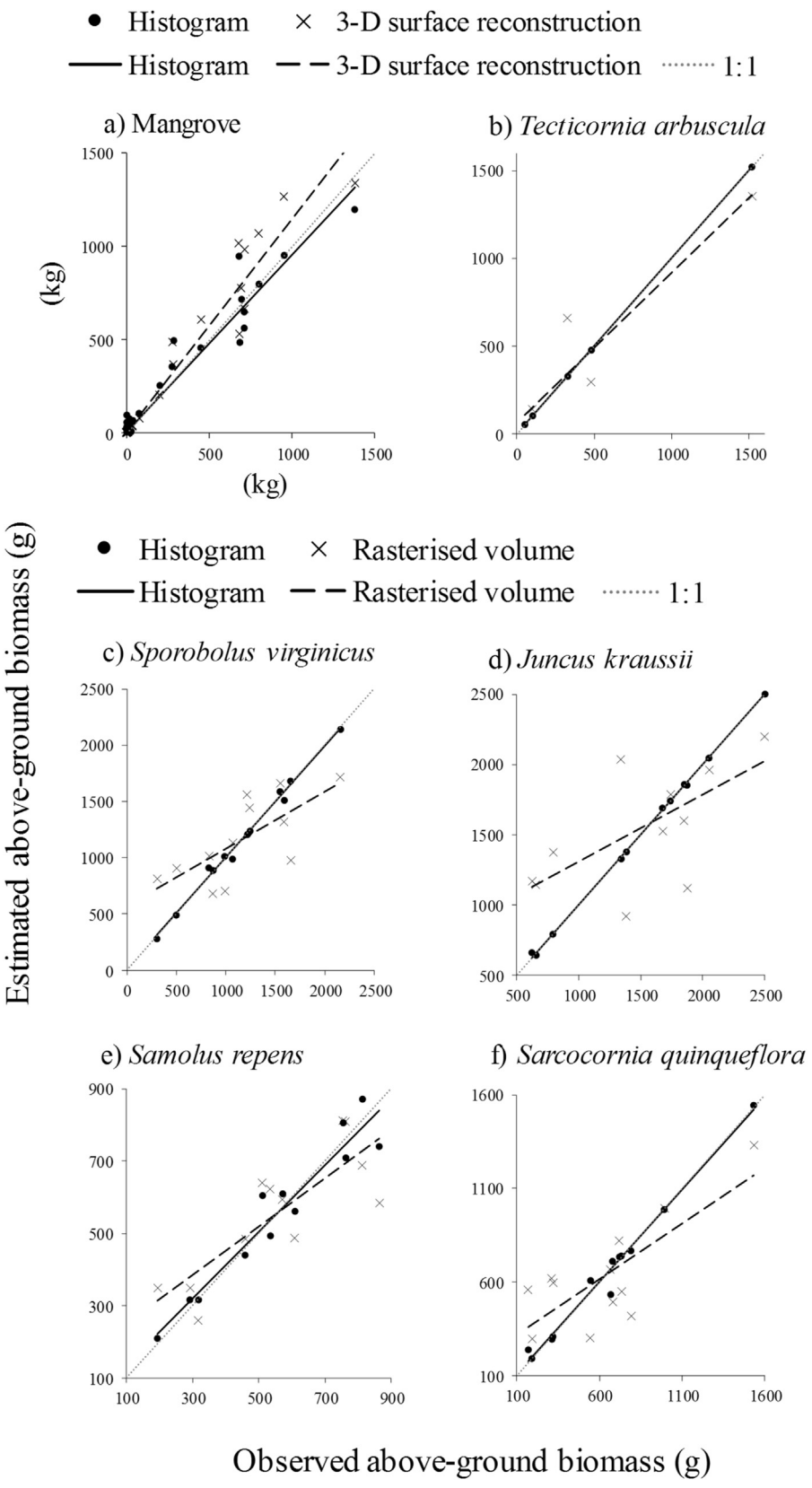

Fig. 6. Model comparison between 3-D surface reconstruction, rasterised volume and point cloud elevation histogram modelling techniques for estimating above-ground biomass. Observed above-ground biomass derived using traditional mangrove allometric and saltmarsh vegetation harvesting techniques. a) mangrove b) *Tecticornia arbuscula* c) *Sporobolus virginicus*, d) *Juncus kraussii*, e) *Samolus repens*, f) *Sarcocornia quinqueflora*. 1:1 line shown for reference.

arbuscula, the estimated AGB of the 3-D surface reconstruction was the average of the two methods employed (Poisson and convex hull).

Overall the point cloud elevation histogram models for mangrove and saltmarsh were more robust than volumetric models. For mangrove 3-D surface reconstruction methods, biomass was overestimated compared to allometric derived biomass estimates. These results are similar to trends in Fig. 4. The 3-D surface reconstruction model and point cloud elevation histogram model had similar r^2 (0.95), however biomass estimates using the 3-D surface reconstruction model were significantly different to the 1:1 line ($p = 0.0001$). For *Tecticornia arbuscula* biomass estimates, the point cloud elevation histogram model was more robust ($r^2 = 0.99$) than the 3-D surface reconstruction model ($r^2 = 0.88$), despite both models being similar to the 1:1 regression ($p = 0.4547$, $p = 0.9977$).

For *Sporobolus virginicus*, *Samolus repens*, *Juncus kraussii* and *Sarcocornia quinqueflora*, r^2 was substantially higher for the point cloud elevation histogram model compared to the rasterised volume model (see Tables 2 and 3). All biomass estimates using the rasterised volume model were significantly different to the 1:1 regression, however differences between the point cloud elevation histogram model and 1:1 regression were insignificant (*Sporobolus virginicus* $p = 0.0053$, $p = 0.6749$, *Samolus repens* $p = 0.0375$, $p = 0.3711$, *Juncus kraussii* $p = 0.0034$, $p = 0.9409$ and *Sarcocornia quinqueflora* $p = 0.0167$, $p = 0.6739$).

4. Discussion

4.1. Synthesis of results

This study applied TLS to demonstrate its effectiveness in determination of biomass in structurally complex wetlands. TLS-derived biomass estimates for mangrove were comparable with biomass estimates derived from traditional allometric techniques, similar to results found elsewhere (Feliciano et al., 2014; Calders et al., 2015; Olagoke et al., 2015). Substantial variability in biomass estimates was established, likely due to structural complexity of temperate *Avicennia marina* (Morrisey et al., 2010; Owers et al., 2016b, in review). Established relationships between biomass and volume using the rasterised volumetric approach for saltmarsh were broadly similar to previous studies (Loudermilk et al., 2009; Eitel et al., 2014; Cooper et al., 2017; Wallace et al., 2017). However, our results suggest that this approach may oversimplify the structural complexity of saltmarsh, and underutilises the information provided by the point cloud. The point cloud elevation histogram model presented in this study provides an alternate approach that utilises all of the information within the point cloud, as opposed to sub-sampling based on specific criteria. Model comparisons show that the point cloud elevation histogram models were more robust than both 3-D surface reconstruction models and rasterised volumetric models, suggesting this method is preferable and should be used in future studies.

4.2. Mangrove biomass from 3-D surface reconstruction models

Above-ground biomass estimates for mangrove vegetation derived from 3-D surface reconstruction models produced similar results to traditional allometric equation estimates. Estimates derived using allometric equations were not significantly different to estimates derived from 3-D surface reconstruction models, however several outliers were identified. These outliers are due to the inability of allometric equations to account for tree measured variables that are outside the normal range. For example, one mangrove individual with a height of 5.5 m had a total stem diameter of 47.2 cm, substantially different from the majority of mangroves with similar height (i.e. total stem diameter 15–30 cm). This resulted in TLS-derived biomass estimates being two-fold greater that the allometric-based estimate. For non-woody estimates of larger mangroves, five of the 30 mangrove individuals were outside the 95% confidence interval using the allometric equation. This may be due to outliers with markedly different tree measured variables, however non-woody compartments of mangroves can have considerable variability and may not correlate to plant growth (Soares and Schaeffer-Novelli, 2005; Kauffman and Donato, 2012).

The majority of large mangrove individual biomass was within the 95% confidence interval, however markedly different biomass estimates occurred in some mangroves, particularly those larger than 5 m in height. Of the 12 mangrove individuals larger than 5 m in height, eight have higher biomass for estimates derived from 3-D surface reconstruction models, with an average of 30% increase. Large older mangroves typically undergo decay and form hollows and cavities (Saenger, 2002), however for woody compartments, TLS-derived estimates assume full density of wood in modelled volume. This has been discussed previously regarding mangrove woody estimates (Olagoke et al., 2015) and may explain why TLS estimates for tall mangrove woody compartments in this study are higher than allometric derived estimates.

Although mangroves in temperate settings have less species diversity than tropical and sub-tropical regions, research suggests that structural complexity is high, influencing above-ground biomass (Owers et al., in review; Morrisey et al., 2010). This may explain why mangrove woody compartment biomass estimates in this study were substantially more variable than previous studies in mangrove forests. Average deviation of TLS-derived biomass estimates from allometric estimates was 20% for mangrove woody compartments. Previous studies in southern Florida and French Guiana suggest up to 90% agreement between TLS-derived estimates and allometric estimates (Feliciano et al., 2014; Olagoke et al., 2015), however, these studies model relatively tall trees (up to 23 m Feliciano et al., 2014, 14–41 m Olagoke et al., 2015) with simple structure (i.e. fairly straight trunks, minimal branching and similar growth forms between juvenile and mature trees). Differences between TLS and allometric biomass estimates in this study may be further exacerbated by variability in growth forms of *Avicennia marina* in temperate settings, particularly in southeast Australia (Owers et al., in review; Saintilan, 1997; Morrisey et al., 2010; Owers et al., 2016b).

Several 3-D surface reconstruction models were tested in this study to determine the optimal model for estimating biomass for wetland vegetation that is structurally complex. Previous studies have used QSMs, or similar geometric shapes (Feliciano et al., 2014; Ishak et al., 2015), to model tree woody compartments with reasonable success (Calders et al., 2013, 2015; Raumonen et al., 2013; Kaasalainen et al., 2014; Hackenberg et al., 2015a; Paynter et al., 2016; Stovall et al., 2017). We expected that the Poisson surface reconstruction model may perform better than QSMs, particularly when tree architecture is complex, as a continuous surface model is created rather than discrete objects. However, our results demonstrate that both QSMs and Poisson surface reconstruction models are appropriate for structurally complex mangrove, whereby differences in volume and biomass estimates was insignificant ($p = 0.9213$).

For non-woody mangrove compartments, small stature mangroves and *Tecticornia arbuscula*, Poisson and convex hull surface reconstruction models produced markedly different volume estimates. Both reconstruction models have been used in previous research with varying success, particularly in reconstruction of small stature plants (Olsoy et al., 2014, 2016; Stovall et al., 2017).

Volume estimates derived using convex hull surface reconstruction models were greater than Poisson surface reconstruction models, however estimates were highly correlated. This was not surprising as Poisson reconstruction is particularly resistant to outliers in the point cloud, whereas convex hull reconstruction ensures the volume estimate encompasses all points (Barber et al., 1996; Kazhdan and Hoppe, 2013; Olsoy et al., 2014). Differences in volume estimates are likely exacerbated by structural complexity of vegetation. However, as volume estimates were highly correlated, biomass estimates for both reconstruction models were not significantly different.

Non-woody biomass has rarely been considered in TLS biomass studies, with many studies focusing on woody compartment biomass (i.e. Belton et al., 2013; Calders et al., 2013, 2015; Raumonen et al., 2013; Kaasalainen et al., 2014; Olagoke et al., 2015). This is likely due to the comparatively lower contribution of non-woody compartment biomass to total biomass, as well as difficulty in modelling the canopy from the point cloud. In this study we provide a method to derive non-woody biomass estimates which can also be applied in a similar fashion to smaller stature plants and shrubs where the woody compartment cannot be delineated and modelled separately. A canopy correction factor for mangrove was applied in Feliciano et al. (2014), assuming non-woody biomass accounted for $20 \pm 10\%$ of total biomass based on estimates from previous research (Clough et al., 1997; Fromard et al., 1998; Komiyama et al., 2005). However non-woody biomass contribution to total biomass can be highly variable, ranging from 2 to 25% in mangrove forests (Fromard et al., 1998, Alongi et al., 2003; Comley and McGuinness, 2005; Bulmer et al., 2016; Hossain et al., 2016). Results from biomass estimates of mangrove in this study suggest that average non-woody biomass contributes $13 \pm 3\%$ of total above-ground biomass. Future studies should include non-woody compartment estimates as current approaches that only focus on woody compartment biomass limit the adoption of TLS for biomass estimates. Furthermore, measuring only woody compartments limits studies to larger trees, and restricts the use of high precision non-destructive approaches for small stature mangroves and other shrub vegetation. This is the first attempt to derive non-woody biomass estimates for mangroves, and subsequently small stature mangrove biomass, using TLS.

In this study we use allometric equations to estimate mangrove biomass as a reference to compare the validity of TLS-derived biomass estimates. However, allometric equations can have considerable uncertainty in estimates, particularly for structurally complex mangroves (Soares and Schaeffer-Novelli, 2005). Recent research by Calders et al. (2015) compared TLS-derived biomass estimates and allometric equation estimates by harvesting 28 trees in a eucalypt forest. Their results suggest that TLS overestimates biomass by 10%, compared to allometric equations which underestimate biomass by 30%. Previous studies in mangrove forests have used allometric equations as a reference to compare TLS-derived biomass estimates (Feliciano et al., 2014; Olagoke et al., 2015), however TLS is yet to be applied where mangrove are subsequently harvested. To verify relationships established in this study (and others) a subset of scanned mangrove should be harvested and compared to TLS approaches for estimating biomass.

4.3. *Tecticornia arbuscula* biomass from 3-D surface reconstruction models

This study is the first to present data on above-ground biomass of *Tecticornia*, and makes the first attempt to model *Tecticornia arbuscula* biomass with TLS-derived volume estimates. Despite limited sample numbers, the methodology used in this study was demonstrated to be useful for non-destructive assessment of *Tecticornia arbuscula* biomass. Our results are consistent with previous studies that used 3-D surface reconstruction models to estimate biomass of shrub vegetation. For example, Olsoy et al. (2014) modelled and harvested 91 sagebrush individuals from the Great Basin USA, demonstrating similar relationships to those found in this study for *Tecticornia arbuscula*. Future research should build upon the results of this study by harvesting an increased number of *Tecticornia arbuscula*, and develop traditional allometric equations and TLS-derived relationships so that above-ground biomass can be estimated confidently using non-destructive techniques. *Tecticornia arbuscula* can be extensive in some estuaries of southeast Australia and represents an important biomass contribution that should be accounted for.

4.4. Rasterised volumetric model for saltmarsh grasses

Saltmarsh vegetation in temperate settings such as southeast Australia is structurally complex, varying with species distribution and stand density (Owers et al., in review; Clarke, 1993; Clarke and Jacoby, 1994). In this study we used the rasterised volumetric model to correlate volume with harvested biomass for four saltmarsh species. Relationships established in this study show variability between species, with r^2 ranging from 0.48 to 0.67. These results are broadly similar to other established relationships for grass and crop species in terrestrial environments ($r^2 = 0.83$: Loudermilk et al. (2009), $r^2 = 0.72–0.79$: Eitel et al. (2014), $r^2 = 0.46–0.57$: Cooper et al. (2017), $r^2 = 0.69–0.75$: Wallace et al. (2017)). We also tested various rasters with different cell sizes and found these similarly varied among species, consistent with previous studies (Eitel et al., 2014; Cooper et al., 2017; Wallace et al., 2017).

The rasterised volumetric approach is a relatively simple technique to obtain volumetric calculations of biomass for grass and crop vegetation that cannot be modelled similarly to woody vegetation. However results from this study suggest that this approach may over-simplify the structural complexity of saltmarsh and under-utilises the information provided by the point cloud. The rasterised volumetric approach assumes full biomass density calculated from the DSM (Loudermilk et al., 2009; Eitel et al., 2014; Greaves et al., 2015; Cooper et al., 2017). Although height may be proportional to biomass for some grass species, this is not the case for saltmarsh. For example substantial variation in biomass can occur between stands of *Juncus kraussii* that have similar height but markedly different density (Owers et al., in review; Clarke and Jacoby, 1994). We demonstrated that the rasterised volumetric approach does not provide the required confidence in biomass estimates for saltmarsh, particularly in areas of high species diversity and variability in density.

4.5. Biomass and point cloud elevation histograms

TLS as a non-destructive method for estimating biomass has received considerable attention due to the large amount of structural information it can provide. Despite equipment and analytical costs being a significant deterrent for adoption of TLS for biomass estimates (Newnham et al., 2012; Eitel et al., 2014; Cooper et al., 2017), current modelling approaches have also discouraged widespread application due to expert knowledge and computational time required, as well as oversimplification of the point cloud (Newnham et al., 2015). The point cloud elevation histogram model presented in this study provides a method that maximises utilisation of the TLS point cloud and applies relatively simple data analysis techniques. Similar approaches have been used in previous research to analyse canopy distribution and biomass of large terrestrial trees with varying success (i.e. Hauglin et al., 2013;

Kankare et al., 2013; Srinivasan et al., 2014; Newnham et al., 2015; Rahman et al., 2017). A preliminary study by Edwards (2016) utilises the point cloud elevation histogram to investigate the relationship between above-ground biomass of two saltmarsh species in the USA. The results from Edwards (2016) show promising capability of using the histogram to model above-ground biomass, however their model approach is complex, site-specific and difficult to replicate elsewhere. The method presented in this study utilises several descriptive parameters from the point cloud elevation histogram to explain above-ground biomass of both mangrove and saltmarsh vegetation. This method is simple but highly effective for both mangrove ($r^2 = 0.95$) and saltmarsh ($r^2 > 0.92$) vegetation.

We propose that future biomass modelling using TLS-derived point clouds should apply the point cloud elevation histogram model demonstrated in this study. Unlike other the 3-D surface reconstruction models and rasterised volumetric approach presented in this study, the point cloud elevation histogram model does not require delineation of woody and non-woody vegetation and can be applied to both mangrove and saltmarsh vegetation. Model comparisons demonstrate that the point cloud elevation histogram models were more robust than both the 3-D surface reconstruction model and rasterised volumetric model. Limited harvest data, due to the conservation status of mangrove and saltmarsh in southeast Australia, required all samples to be used in model generation, and further validation could be achieved by comparison of modelled biomass estimates with independently harvested biomass.

5. Conclusions

This study demonstrates that TLS is a reliable non-destructive method for estimating biomass of structurally complex coastal wetland vegetation. Our results demonstrate that current volumetric modelling approaches for estimating TLS-derived biomass are comparable to traditional mangrove allometrics and saltmarsh harvesting. However, volumetric modelling approaches oversimplify vegetation structure by under-utilising the large amount of structural information provided by the point cloud. As a result many studies using TLS have focused on estimating woody compartment biomass of large trees, overlooking non-woody compartment biomass and shrub biomass, which can account for considerable carbon storage over large extents. Current modelling approaches that focus only on woody compartment biomass limit the adoption of TLS for biomass estimates. We propose that future biomass modelling using TLS-derived point clouds should apply the point cloud elevation histogram model demonstrated in this study. This approach maximises utilisation of the information provided by the point cloud, avoiding over-simplification, reducing computational time, and does not require extensive modelling to extract volume. Furthermore, the point cloud elevation histogram model can be applied to both mangrove and saltmarsh vegetation. The research presented here advances modelling methods using TLS as a non-destructive method for estimating biomass in coastal wetlands.

Acknowledgements

The authors would like to thank Brent Peterson, Jeffrey Kelleway, Stephen Brooks, Kate Owers, Thomas Doyle and Kieran Northam for their assistance with field data collection. We would also like to thank the NSW National Parks and Wildlife Service, NSW Department of Primary Industries (Fisheries) and the Victorian Department of Environment, Land, Water and Planning for supporting access to field sites. Harvesting of vegetation was undertaking in accordance with the Office of Environment and Heritage Scientific license SL101724. This research has been conducted with the support of the University of Wollongong Global Challenges Program, the Australian Government Research Training Program Scholarship award to CO, and Australian Research Council Future Fellowship awarded to KR (FT130100532). The authors have no competing interests to declare.

Appendix A. Supplementary data

Supplementary data related to this article can be found at https://doi.org/10.1016/j.ecss.2018.02.027.

Supplementary video related to this article can be found at https://doi.org/10.1016/j.ecss.2018.02.027.

References

Adam, P., 1990. Saltmarsh Ecology. Cambridge University Press, Cambridge, UK.
Aertsen, W., Kint, V., van Orshoven, J., Ozkan, K., Muys, B., 2010. Comparison and ranking of different modelling techniques for prediction of site index in Mediterranean mountain forests. Ecol. Model. 221 (8), 119–1130.
Alongi, D.M., 2014. Carbon cycling and storage in mangrove forests. Ann. Rev. Mar. Sci. 6, 195–219.
Alongi, D.M., Clough, B.F., Dixon, P., Tirendi, F., 2003. Nutrient partitioning and storage in arid-zone forests of the mangroves *Rhizophora stylosa* and *Avicennia marina*. Trees (Berl.) 17, 51–60.
Alongi, D.M., Murdiyarso, D., Fourqurean, J.W., Kauffman, J.B., Hutahaean, A., Crooks, S., Lovelock, C.E., Howard, J., Herr, D., Fortes, M., Pidgeon, E., Wagey, T., 2015. Indonesia's blue carbon: a globally significant and vulnerable sink for seagrass and mangrove carbon. Wetl. Ecol. Manag. 24, 3–13.
Barber, C.B., Dobkin, D.P., Huhdanpaa, H., 1996. The quickhull algorithm for convex hulls. ACM Trans. Math Software 22, 469–483.
Barbier, E.B., Hacker, S.D., Kennedy, C., Koch, E.W., Stier, A.C., Silliman, B.R., 2011. The value of estuarine and coastal ecosystem services. Ecol. Monogr. 81 (2), 169–193.
Belton, D., Moncrieff, S., Chapman, J., 2013. Processing tree point clouds using Gaussian mixture models. ISPRS Ann. Photogram., Remote Sens. Spatial Inf. Sci. 2, 43–48.
Bonham, C.D., 2013. Measurements for Terrestrial Vegetation, second ed. Wiley-Blackwell, West Sussex, UK.
Bulmer, R.H., Schwendenmann, L., Lundquist, C.J., 2016. Allometric models for estimating aboveground biomass, carbon and nitrogen stocks in temperate *Avicennia marina* forests. Wetlands 36 (5), 841–848.
Calders, K., Newnham, G., Herold, M., Murphy, S., Culvenor, D., Raumonen, P., Burt, A., Armston, J., Avitabile, V., Disney, M., 2013. Estimating above Ground Biomass from Terrestrial Laser Scanning in Australian Eucalypt Open Forest. SilviLaser, Beijing, China, 9–11 Oct. 2013.
Calders, K., Newnham, G., Burt, A., Murphy, S., Raumonen, P., Herold, M., Culvenor, D., Avitabile, V., Disney, M., Armston, J., Kaasalainen, M., 2015. Nondestructive estimates of above-ground biomass using terrestrial laser scanning. Meth. Ecol. Evol. 6, 198–208.
Chave, J., Rejou-Mechain, M., Burquez, A., Chidumayo, E., Colgan, M.S., Delitti, W.B.C., Duque, A., Eid, T., Fearnside, P.M., Goodman, R.C., Henry, M., Martinex-Yrizar, A., Mugasha, W.A., Muller-Landau, H.C., Mencuccini, M., Nelson, B.W., Ngomanda, A., Nogueira, E.M., Ortiz-Malavassi, E., Pelissier, R., Ploton, P., Ryan, C.M., Saldarriaga, J.G., Vielledent, G., 2014. Improved allometric models to estimate the aboveground biomass of tropical trees. Global Change Biol. 20, 3177–3190.
Clarke, P.J., 1993. Mangrove, saltmarsh and peripheral vegetation of Jervis Bay. Cunninghamia 31, 231–253.
Clarke, P.J., Jacoby, C.A., 1994. Biomass and above-ground productivity of saltmarsh plants in south-eastern Australia. Mar. Freshw. Res. 45, 1521–1528.
Clough, B.F., Dixon, P., Dalhaus, O., 1997. Allometric relationships for estimating biomass in multi-stemmed mangrove trees. Aust. J. Bot. 45, 1023–1031.
Comley, B.W.T., McGuinness, K.A., 2005. Above- and below-ground biomass, and allometry, of four common northern Australian mangroves. Aust. J. Bot. 53 (5), 431–436.
Cooper, S.D., Roy, D.P., Schaaf, C.B., Paynter, I., 2017. Examination of the potential of terrestrial laser scanning and structure-from-motion photogrammetry for rapid nondestructive field measurement of grass biomass. Rem. Sens. 9, 1–13.
Craft, C., 2013. Emergent macrophyte biomass production. In: DeLaune, R.D., Reddy, K.R., Richardson, C.J., Megonigal, J.P. (Eds.), Methods in Biogeochemistry of Wetlands. Soil Science Society of America, pp. 137–153.
Duarte, C.M., Middelburg, J.J., Caraco, N., 2005. Major role of marine vegetation on the oceanic carbon cycle. Biogeosciences 2, 1–8.
Edwards, J.D., 2016. Applicability of LiDAR Technology in Saltmarshes: Landscape-scale Predictive Models to Local-scale Biomass Estimation. Master's thesis. University of South Carolina. Retrieved from: http://scholarcommons.sc.edu/etd/3550.
Eitel, J.U.H., Magney, T.S., Vierling, L.A., Brown, T.T., Huggins, D.R., 2014. LiDAR based

biomass and crop nitrogen estimates for rapid, non-destructive assessment of wheat nitrogen status. Field Crop. Res. 159, 21–32.
Estrada, G.C.D., Soares, M.L.G., Santos, D.M.C., Fernandez, V., de Almeida, P.M.M., de Medeiros Estevam, M.R., Machado, M.R.O., 2014. Allometric models for above-ground biomass estimation of the mangrove *Avicennia schaueriana*. Hydrobiologia 734, 171–185.
Ewel, K.C., Twilley, R.R., Ong, J.E., 1998. Different kinds of mangrove forest provide different goods and services. Global Ecol. Biogeogr. Lett. 7, 83–94.
Fabozzi, F.J., Focardi, S.M., Rachev, S.T., Arshanapalli, B.G., 2014. The Basics of Financial Econometrics: Tools, Concepts, and Asset Management Applications. Appendix E Model Selection Criterion: AIC and BIC. John Wiley and Sons.
Feliciano, E.A., Wdowinski, S., Potts, M.D., 2014. Assessing mangrove above-ground biomass and structure using terrestrial laser scanning: a case study in the everglades national park. Wetlands 34 (5), 955–968.
Fromard, F., Puig, H., Mougin, E., Marty, G., Betoulle, J.L., Cadamuro, L., 1998. Structure, above-ground biomass and dynamics of mangrove ecosystems: new data from French Guiana. Oecologia 115, 39–53.
Gibbs, H.K., Brown, S., Niles, J.O., Foley, J.A., 2007. Monitoring and estimating tropical forest carbon stocks: making REDD a reality. Environ. Res. Lett. 2, 1–13.
Greaves, H.E., Vierling, L.A., Eitel, J.U., Boelman, N.T., Magney, T.S., Prager, C.M., Griffin, K.L., 2015. Estimating aboveground biomass and leaf area of low-stature arctic shrubs with terrestrial lidar. Remote Sens. Environ. 164, 26–35.
Hackenberg, J., Wassenberg, M., Spiecker, H., Sun, D., 2015a. Non destructive method for biomass prediction combining TLS derived tree volume and wood density. Forests 6, 1274–1300.
Hackenberg, J., Spiecker, H., Calders, K., Disney, M., Raumonen, P., 2015b. SimpleTree—an efficient open source tool to build tree models from TLS clouds. Forests 6, 4245–4294.
Hauglin, M., Dibdiakova, J., Terje, G., Naesset, E., 2013. Estimating single-tree branch biomass of Norway spruce by airborne laser scanning. ISPRS J. Photogrammetry Remote Sens. 79, 147–156.
Hossain, M., Shaikh, M.A., Saha, C., Abdullah, S.M.R., Saha, S., Siddique, M.R.H., 2016. Above-ground biomass, nutrients and carbon in *Aegiceras corniculatum* of the Sundarbans. Open J. For. 6, 72–81.
Howard, J., Hoyt, S., Isensee, K., Pidgeon, E., Telszewski, M., 2014. Coastal Blue Carbon: Methods for Assessing Carbon Stocks and Emissions Factors in Mangroves, Tidal Salt Marshes, and Seagrass Meadows. Conservation International, Intergovernmental Oceanographic Commission of UNESCO, International Union for Conservation of Nature, Arlington, Virginia, USA.
Ishak, N.I., Bakar, M.A.A., Rahman, M.Z.A., Rasib, A.W., Kanniah, K.D., Shin, A.L.M., Razak, K.A., 2015. Estimating single tree stem and branch biomass using terrestrial laser scanning. Jurnal Teknologi 26, 59–67.
Kaasalainen, S., Krooks, A., Liski, J., Raumonen, P., Kaartinen, H., Kaasalainen, M., Puttonen, E., Anttila, K., Mäkipää, R., 2014. Change detection of tree biomass with terrestrial laser scanning and quantitative structure modelling. Rem. Sens. 6, 3906–3922.
Kankare, V., Holopainen, M., Vastaranta, M., Puttonen, E., Yu, X., Hyyppa, J., Vaaja, M., Hyyppa, H., Alho, P., 2013. Individual tree biomass estimation using terrestrial laser scanning. ISPRS J. Photogrammetry Remote Sens. 75, 64–75.
Kauffman, J.B., Donato, D.C., 2012. Protocols for the Measurement, Monitoring and Reporting of Structure, Biomass and Carbon Stocks in Mangrove Forests. Working Paper 86. CIFOR, Bogor, Indonesia.
Kazhdan, M., Hoppe, H., 2013. Screened Poisson surface reconstruction. ACM Trans. Graph. 32 (3), 1–13.
Kelleway, J.J., Saintilan, N., Macreadie, P.I., Skilbeck, C.G., Zawadzki, A., Ralph, P.J., 2016. Seventy years of continuous encroachment substantially increases 'blue carbon' capacity as mangroves replace intertidal salt marshes. Global Change Biol. 22 (3), 1097–1109.
Kelleway, J.J., Serrano, O., Baldock, J., Cannard, T., Lavery, P., Lovelock, C.E., Macreadie, P.I., Masqué, P., Saintilan, N., Steven, A.D.L., 2017. Technical Review of Opportunities for Including Blue Carbon in the Australian Government's Emissions Reduction Fund. CSIRO, Australia.
Komiyama, A., Poungparn, S., Kato, S., 2005. Common allometric equations for estimating the tree weight of mangroves. J. Trop. Ecol. 21, 471–477.
Komiyama, A., Ong, J.E., Poungparn, S., 2008. Allometry, biomass, and productivity of mangrove forests: a review. Aquat. Bot. 89 (2), 128–137.
Lee, Primavera J.H., Dahdouh-Guebas, F., McKee, K., Bosire, J.O., Cannicci, S., Diele, K., Fromard, F., Koedam, N., Marchand, C., Mendelssohn, I., Mukherjee, N., Record, S., 2014. Ecological role and services of tropical mangrove ecosystems: a reassessment. Global Ecol. Biogeogr. 23, 726–743.
Loudermilk, E.L., Hiers, J.K., O'Brien, J.J., Mitchell, R.J., Singhania, A., Fernandez, J.C., Cropper, W.P., Slatton, K.C., 2009. Ground-based lidar: a novel approach to quantify fine-scale fuelbed characteristics. Int. J. Wildland Fire 18, 676–685.
Macreadie, P.I., Ollivier, Q.R., Kelleway, J.J., Serrano, I., Carnell, P.E., Ewers Lewis, C.J., Atwood, T.B., Sanderman, J., Baldock, J., Connolly, R.M., Duarte, C.M., Lavery, P.S., Steven, A., Lovelock, C.E., 2017. Carbon sequestration by Australian tidal marshes. Sci. Rep. 7, 1–10.
McLeod, E., Chmura, G.L., Bouillon, S., Salm, R., Bjork, M., Duarte, C.M., Lovelock, C.E., Schlesinger, W.H., Silliman, B.R., 2011. A blueprint for blue carbon: toward an improved understanding of the role of vegetated coastal habitats in sequestering CO_2. Front. Ecol. Environ. 9, 552–560.
Morrisey, D.J., Swales, A., Dittman, S., Morrison, M.A., Lovelock, C.E., Beard, C.M., 2010. The ecology and management of temperate mangroves. Oceanogr. Mar. Biol. Annu. Rev. 48, 43–160.
Newnham, G.J., Armston, J.D., Muir, J., Goodwin, N., Tindall, D., Culvenor, D., Püschel, P., Nyström, M., Johansen, K., 2012. Evaluation of Terrestrial Laser Scanners for Measuring Vegetation Structure. CSIRO Sustainable Agriculture Flagship. Manuscript ID: EP124571.
Newnham, G.J., Armston, J.D., Calders, K., Disney, M.I., Lovell, J.L., Schaaf, C.B., Strahler, A.H., Danson, F.M., 2015. Terrestrial laser scanning for plot-scale forest measurement. Curr. For. Rep. 1, 239–251.
Olagoke, A., Proisy, C., Feret, J., Blanchard, E., Fromard, F., Mehlig, U., de Menezes, M.M., dos Santos, V.F., Berger, U., 2015. Extended biomass allometric equations for large mangrove trees from terrestrial LiDAR data. Trees (Berl.) 30 (3), 935–947.
Olsoy, P.J., Glenn, N.F., Clark, P.E., Derryberry, D.R., 2014. Aboveground total and green biomass of dryland shrub derived from terrestrial laser scanning. ISPRS J. Photogrammetry Remote Sens. 88, 166–173.
Osloy, P.J., Mitchell, J.J., Levia, D.F., Clark, P.E., Glenn, N.F., 2016. Estimation of big sagebrush leaf area index with terrestrial laser scanning. Ecol. Indicat. 61, 815–821.
Owers, C.J., Rogers, K., Mazumder, D., Woodroffe, C.D., 2016a. Spatial variation in carbon storage: a case study for Currambene Creek, NSW, Australia. In: Vila-Concejo, A., Bruce, E., Kennedy, D.M., McCarroll, R.J. (Eds.), Proceedings of the 14th International Coastal Symposium (Sydney, Australia), vol. 75. Journal of Coastal Research, pp. 1297–1301.
Owers, C.J., Rogers, K., Woodroffe, C.D., 2016b. Identifying spatial variability and complexity in wetland vegetation using and object-based approach. Int. J. Rem. Sens. 37 (18), 4296–4316.
Owers, C.J., Rogers, K., Woodroffe, C.D., in review. Spatial variation of above-ground carbon storage in temperate coastal wetlands. Estuar. Coast Shelf Sci..
Paynter, I., Saenz, E., Genest, D., Peri, F., Erb, A., Li, Z., Wiggin, K., Muir, J., Raumonen, P., Schaaf, E.S., Strahler, A., Schaaf, C., 2016. Observing ecosystems with lightweight, rapid-scanning terrestrial lidar scanners. Remote Sens. Ecol. Conserv. 2 (4), 174–189.
Pitt, M.A., Myung, J., 2002. When a good fit can be bad. Trends Cognit. Sci. 6, 421–425.
Rahman, M.Z.A., Bakar, M.A.A., Razak, K.A., Rasib, A.W., Kanniah, K.D., Kadir, W.H.W., Omar, H., Faidi, A., Kassim, A.R., Latif, Z.A., 2017. Non-destructive, laser-based individual tree aboveground biomass estimation in a tropical rainforest. Forests 8, 1–22.
Raumonen, P., Kaasalainen, M., Akerblom, M., Kaasalainen, S., Kaartinen, H., Vastaranta, M., Holopainen, M., Disney, M., Lewis, P., 2013. Fast automatic precision tree models from terrestrial laser scanner data. Rem. Sens. 5, 491–520.
Roy, P.S., Williams, R.J., Jones, A.R., Yassini, I., Gibbs, P.J., Coates, B., West, R.J., Scanes, P.R., Hudson, J.P., Nichol, S., 2001. Structure and function of south-east Australian estuaries. Estuarine, Estuar. Coast Shelf Sci. 53, 351–384.
Saenger, P., 2002. Mangrove Ecology, Silviculture and Conservation. Springer, Berlin, Germany.
Saintilan, N., 1997. Above- and below-ground biomasses of two species of mangrove on the Hawkesbury River estuary, New South Wales. Mar. Freshw. Res. 48, 147–152.
Saintilan, N., 2009. Biogeography of Australian saltmarsh plants. Austral Ecol. 34, 929–937.
Sainty, G., Hosking, J., Carr, G., Adam, P., 2012. Estuary Plans and What's Happening to Them in South-east Australia. Sainty Books, Australia.
Soares, M.L.G., Schaeffer-Novelli, Y., 2005. Above-ground biomass of mangrove species: I. Analysis of models. Estuar. Coast Shelf Sci. 65, 1–18.
Sprugel, D.G., 1983. Correcting for bias in log-transformed allometric equations. Ecology 64 (1), 209–210.
Srinivasan, S., Popescu, S.C., Eriksson, M., Sheridan, R.D., Ku, N., 2014. Multi-temporal terrestrial laser scanning for modeling tree biomass change. For. Ecol. Manag. 318, 304–317.
Stovall, A.E.L., Vorster, A.G., Anderson, R.S., Evangelista, P.H., Shugart, H.H., 2017. Non-destructive aboveground biomass estimation of coniferous trees using terrestrial LiDAR. Remote Sens. Environ. 200, 31–42.
Sutton-Grier, A.E., Moore, A., 2016. Leveraging carbon services of coastal ecosystems for habitat protection and restoration. Coast. Manag. 44 (3), 259–277.
Thursby, G., Chintala, M., Stetson, D., Wigand, C., Champlin, D., 2002. A rapid, non-destructive method for estimating aboveground biomass of salt marsh grasses. Wetlands 22 (3), 626–630.
Twilley, R.R., Chen, R.H., Hargis, T., 1992. Carbon sinks in mangroves and their implications to carbon budget of tropical coastal ecosystems. Water Air Soil Pollut. 64, 265–288.
Wallace, L., Hillman, S., Reinke, K., Hally, B., 2017. Non-destructive estimation of above-ground surface and near-surface biomass using 3D terrestrial remote sensing techniques. Meth. Ecol. Evol. 8 (11), 1607–1616.
Yando, E.S., Osland, M.J., Willis, J.M., Day, R.H., Krauss, K.W., Hester, M.W., 2016. Salt marsh-mangrove ecotones: using structural gradients to investigate the effects of woody plant encroachment on plant–soil interactions and ecosystem carbon pools. J. Ecol. 104 (4), 1020–1031.
Zelder, J.B., Kercher, S., 2005. Wetland resources: status, trends, ecosystem services, and restorability. Annu. Rev. Environ. Resour. 30, 39–74.